Design, Construction, and Calibration of a Portable Boundary Layer Wind Tunnel for Field Use

R. S. Van Pelt, T. M. Zobeck, M. C. Baddock, J. J. Cox

Abstract. *Wind erosion is a natural process that has formed landscapes but threatens sustainable agriculture in many locations. Wind tunnels have been used for several decades to study wind erosion processes. Portable wind tunnels offer the advantage of testing natural surfaces in the field, but they must be carefully designed to ensure that a logarithmic boundary layer is formed and that wind erosion processes may develop without interference from the tunnel structures. Although large portable tunnels often meet the aerodynamic criteria, their size and transportation requirements often limit the locations where they may be employed. We designed and built a self-contained portable wind tunnel that is easily transported on a tandem-axle trailer and pulled with a pickup truck. The wind tunnel uses a centrifugal blower, a flow-conditioning section with optional abrader material feed, and a 1 m tall and 0.5 m wide working section that can vary in length from 2 m to 6 m. The maximum wind velocity attainable is 18.7 m s^{-1} although a mid-height centerline velocity of 12.6 m s^{-1} is normally used for field testing of natural surfaces. Based on measured wind velocity profiles in the tunnel working section, a conservative estimate of boundary layer depth within the working section is 0.5 m. Even though no wind tunnel can truly duplicate the scale and variability of the forces that drive wind erosion, tunnels such as this one with deeply developed boundary layers offer reasonable estimates of dust emissions and erodibilities of natural surfaces. This wind tunnel has been used to test rangeland and cropped surfaces in several locations and has provided reliable and useable soil erodibility and dust emission data.*

Keywords. *Boundary layer, Dust emission, Erodibility, Field studies, Wind erosion, Wind tunnel.*

Wind erosion refers to the detachment, transport, and deposition of sediment or surface soils by wind. This wind-driven movement of soil and sediment has been occurring for eons, as evidenced by the aeolian cross-bedding seen in sandstone bedrock, deep loess deposits, and large stabilized and unstabilized dune fields in many parts of the world. In spite of the natural occurrence of wind erosion, it is considered a soil-degrading process that affects over 500 million ha of land worldwide and creates between 500 and 5000 Tg of fugitive dust annually (Grini et al., 2003). Wind erosion degrades soil by preferentially removing the fine soil particles that contain most of the soil organic carbon and plant nutrients (Zobeck and Fryrear, 1986; Van Pelt and Zobeck, 2007).

Much of what we know about wind erosion comes from wind tunnel-based investigations. The seminal work of Ralph Bagnold (1941) was largely done in a stationary suction-type wind tunnel of 9 m length. Wind tunnels allow control over the wind and surface parameters, and much more work can be accomplished in a given amount of time. Other early wind erosion investigators used wind tunnels to assess the erodibility of soil surfaces without organic residues based on the texture of the soil and relative abundance of non-erodible aggregates on the surface (Chepil, 1950). Large laboratory wind tunnels have been used to develop sufficiently detailed understanding of the controlling factors of wind erosion, allowing predictive models such as the Wind Erosion Equation (WEQ; Woodruff and Siddoway, 1965) and, more recently, the Wind Erosion Prediction System (WEPS; Hagen, 2004; Hagen et al., 1999) to be developed.

Stationary wind tunnels are still widely used for aeolian research today and have been used to investigate wind erosion controlling factors and effects from single grain scale (Huang et al., 2006) through soil surface scale (Kohake et al., 2010) to landscape scale (Offer and Goossens, 1995). Wind tunnels offer a convenient venue to study electrostatic interactions of particles and electrical fields generated by wind-driven soil particles (Zheng et al., 2003). Wind tunnels have also been used to study abrasion effects of wind-driven sand on building materials (Liu et al., 2003), abrasion effects on crop plants (Baker, 2007), abrasion of bare crusted surfaces (Zobeck, 1991) and surfaces with microphytic crusts (McKenna-Neumann and Maxwell, 1999) and to compare and calibrate instrumentation for field studies (Goossens and Offer, 2000; Van Pelt et al., 2009).

Fugitive dust is the most visible evidence of wind erosion, and stationary wind tunnels have been used to study dust emissions from eroding surfaces. The dependence of mineral dust production on sandblasting of soil crusts and aggregates

Submitted for review in January 2010 as manuscript number SW 8401; approved for publication by the Soil & Water Division of ASABE in August 2010.

The use of trade names or commercial products is solely for the purpose of providing specific information and does not imply recommendation or endorsement by USDA-ARS or exclusion of other similar products.

The authors are **R. Scott Van Pelt,** Soil Scientist, **Ted M. Zobeck,** Soil Scientist, **Matthew C. Baddock,** Post-Doctoral Research Associate, USDA-ARS Wind Erosion and Water Conservation Research Unit. Cropping Systems Research Laboratory, Lubbock, Texas; and **Jenny Jo Cox,** Former Graduate Research Assistant, Texas Tech University and USDA-ARS Wind Erosion and Water Conservation Research Unit. Cropping Systems Research Laboratory, Lubbock, Texas. **Corresponding author:** R. Scott Van Pelt, USDA-ARS Wind Erosion and Water Conservation Research Unit, Big Spring Field Station, 302 W. I-20, Big Spring, TX 79720; phone: 432-263-0293, ext 103; fax: 432-263-3154; e-mail: scott.vanpelt@ars.usda.gov.

Table 1. Summary of previous and present portable wind tunnel designs, dimensions, maximum wind speed (U_{max}) reported, and boundary layer thickness.

Reference	Tunnel Design	Width (m)	Height (m)	Length (m)	U_{max} (m s^{-1})	Boundary Layer (m)
Zingg (1951a)	Pusher	0.91	0.91	9.12	17	0.23
Armbrust and Box (1967)	Suction	0.91	1.22	7.32	18	--
Gillette (1978b)	Suction	0.15	0.15	3.01	7	--
Fryrear (1984, 1985)	Pusher	0.60	0.90	7.00	20	0.15
Nickling and Gillies (1989)	Suction	1.00	0.75	11.90	15	>0.2
Raupach and Leys (1990)	Pusher	1.20	0.90	4.20	14	0.40
Pietersma et al. (1996)	Pusher	1.00	1.20	5.60	>20	>1.0
Leys et al. (2002)	Suction	0.05	0.10	1.00	19	--
Maurer et al. (2006)	Suction	0.60	0.70	9.40	15	--
Fister and Ries (2009)	Pusher	0.70	0.70	3.00	8	0.20
This article	Pusher	0.50	1.00	6.00	18.7	0.50

has been investigated in stationary wind tunnels (Gillette, 1978a; Rice and McEwan, 2001). Amante-Orozco and Zobeck (2002) investigated the effect of calcium carbonate content on the production of aeolian dust in a stationary suction-type wind tunnel. Complex and vegetated surfaces have been studied using stationary laboratory wind tunnels (Kim et al., 2000). More recently, Roney and White (2006) used the same stationary wind tunnel as Kim et al. (2000) to study PM_{10} emission rates for many soils from Death Valley, a dust source area in southern California.

History of Portable Wind Tunnels

In spite of their utility in wind erosion research, stationary wind tunnels have limitations, especially in the assessment of natural soil surfaces for erodibility and dust emissions. Over the last half-century or so, portable tunnels used in the field have been used to measure soil erodibility, the effects of surface characteristics and cover on soil erodibility, and dust emissions from eroding surfaces (Pietersma et al., 1996). Zingg (1951a) was the first to document the design and construction of a portable wind tunnel for field use, and this tunnel was based on seven practical criteria that will be listed later. This wind tunnel was used to test the erodibility of field surfaces (Zingg, 1951b) and to determine roughness and drag from pressure differentials from the beginning to the end of the tunnel (Zingg and Woodruff, 1951). Armbrust and Box (1967) designed and built a pusher-type portable wind tunnel to test the susceptibility of crops to abrasion from saltating particles. Gillette (1978b) constructed a small suction-type portable tunnel to test the threshold velocities of natural surfaces compared with disturbed surfaces and sieved soils. Another very small suction-type wind tunnel has been tested for use in determining relative dust emission rates from a range of iron ores and road surfaces (Leys et al., 2002).

In Australia, Raupach and Leys (1990) built a truck-mounted portable wind tunnel and tested two tunnel cross-section shapes before determining the rectangular cross-section to be superior. They further noted the importance of flow conditioning upstream of the test section and stated aerodynamic criteria for portable wind tunnel design, adding new technical considerations to the practical ones proposed by Zingg (1951a). This wind tunnel has been used to assess the erodibility of bare cultivated and uncultivated soil (Leys and Raupach, 1991), the effects of disturbance on the erodibility of cryptogamic crusts (Leys and Eldridge, 1998), and the injury and recovery of narrow-leaf lupin resulting from saltating particles (Bennell et al., 2007).

Fryrear (1984, 1985) built a pusher-type portable wind tunnel to test the effects of oriented and random roughness elements on soil erodibility. This wind tunnel depended on a small tractor and independent transmission for motive power, thus requiring a large truck and trailer for transportation. Perhaps the largest of the portable wind tunnels built to date is a suction-type tunnel with a 12 m long working section. This tunnel has been used in North America and Africa to determine the erodibilities of natural crusted surfaces (Nickling and Gillies, 1989; Houser and Nickling, 2001a, 2001b; Macpherson et al., 2008). A pusher-type portable wind tunnel with a trailer-mounted fan and a hydraulic lift arm on a heavy truck for moving the assembled tunnel section has been used to assess dust emissions from natural surfaces of loess soils with and without surface ground cover (Pietersma et al., 1996; Saxton et al,. 2000; Chandler et al., 2005; Sharratt, 2007; Copeland et al., 2009). More recently, two very different portable field wind tunnels built by German researchers have been field calibrated (Maurer et al., 2006) or used to assess the effects of livestock trampling and field tillage on soil erodibility (Fister and Ries, 2009). A summary of portable field wind tunnels, the dimensions of their working sections, the maximum wind velocities developed, and reported boundary layer depths is presented in table 1.

Design Criteria and Considerations

Zingg (1951a) proposed seven practical criteria to consider when designing and building a portable wind tunnel for field use. These criteria are listed below;

1. The wind tunnel must be capable of producing an air stream free of general rotation and of known and steady characteristics.
2. It must provide easy and positive control of a range of wind velocities and forces common to the natural wind.
3. It must be durable.
4. It must be safe to use.
5. It should have sufficient size to afford free movement and representative sampling of eroding materials over field surfaces.
6. It must have ready portability.
7. It should be light in weight and amenable to quick and positive assemblage and dismantling.

He further stated that he used commercially available equipment when possible.

Raupach and Leys (1990) suggested six aerodynamic criteria that should be considered in addition to Zingg's practical criteria. Their aerodynamic criteria are listed below:

1. The flow must reproduce the logarithmic wind speed profile in the natural atmosphere, thus ensuring realistic aerodynamic forces on saltating grains.
2. The surface shear stress must scale correctly with the wind speed above the surface so that realistic aerodynamic forces act on grains of all sizes at the surface.
3. The vertical turbulence intensity and scale in the region close to the ground must be realistic, ensuring that vertical turbulent dispersion of suspended grains is properly modeled.
4. The flow must be spatially uniform to avoid local scouring by anomalous regions of high surface stress.
5. Gusts should be simulated in the tunnel due to the fact that higher shear stress is required to initiate erosion than to sustain it.

Raupach and Leys (1990) noted that criteria 1 to 4 are all satisfied if the flow near the ground surface is a well developed equilibrium boundary layer sufficiently deep to contain particle motion in the inner region where the mean wind speed profile is logarithmic and uniform over the eroding area. The logarithmic wind speed profile over a surface has been described for neutral atmospheric stability by:

$$U_z = (u_*/k) \ln(z/z_o) \quad (1)$$

where U_z is the wind speed at height z above the surface, u_* is the friction velocity, z_o is the aerodynamic roughness length of the underlying surface, and k is the von Karman constant, usually taken to be approximately 0.4. Criterion 5 requires turbulence with length scales greater than the dimensions of the tunnel and cannot be naturally generated by shear forces within either the flow-conditioning or working sections of the tunnel. Raupach and Leys (1990) tried to simulate gustiness using mechanical interruption of flow in the flow-conditioning section of the tunnel. However, the turning vane with which they tried to simulate gusts reduced the mean wind speed in the tunnel but did not increase vertical turbulence.

Mehta (1977) stated that "the design of a blower-driven air tunnel...is a combination of art, science, and common sense, the last being the most essential. It is difficult and unwise to predict firm rules for tunnel design." Wind tunnels are composed of a motive force (fan or blower) that induces the flow; a flow-conditioning section or intake diffuser that straightens, limits eddy size, and otherwise modifies the flow; and a test or working section that allows the modified flow to interact with the soil surface. These are the essential elements, and many designs incorporate additional elements, including flow tripping fences and spires to deepen the boundary layer thickness, abrader feeders and regulators to initiate saltation upstream of the working section, and instrumentation including profiling anemometers and sediment samplers of many designs. In almost all cases, portable wind tunnel designs are unique and highly influenced by their intended use.

The fans and blowers employed for wind tunnels are of primarily two types. Axial fans are composed of pitched blades, either fixed or adjustable, arranged radially around the axis of rotation, which is generally aligned with the axis of flow through the tunnel. Although axial fans are highly efficient at inducing flow, the problem of flow spiraling must be addressed (Mehta and Bradshaw, 1979). Centrifugal fans have fixed pitch blades or impellers that are arranged parallel to the axis of rotation at the circumference of a blower cage. The axis of rotation is usually normal to the direction of flow down the tunnel. Centrifugal fans tend to be more flexible with respect to design, create less spiraling in the flow, and are more steady and efficient over a variety of flows. The impellers may be radial, forward facing, or backward facing. Backward-facing impellers provide the highest efficiency in centrifugal blowers (Mehta and Bradshaw, 1979).

Many portable wind tunnels are too compact for adequate flow conditioning. This shortcoming is particularly unfortunate because flow considerations are the most important factor in the successful operation of the tunnel (Raupach and Leys, 1990). Hagen (2001) noted that the tunnel may not reach transport capacity or may overshoot the true transport capacity at some distance into the test section if flow conditioning upwind of the working section is inadequate. Roney and White (2006) stated that wind tunnel height may limit the amount of upward mixing during strong turbulent diffusion.

Tunnel height affects the depth of the boundary layer that may be formed in the wind tunnel test section. Upper limits of the Froude number F have been proposed of from 10 (White and Mounla, 1991) to 20 (Pietersma et al., 1996). The Froude number is defined by:

$$F = U^2/gH \quad (2)$$

where U is the tunnel design wind speed, g is the acceleration due to gravity, and H is the tunnel height. Maurer et al. (2006) recommended having a well developed boundary layer with a logarithmic wind speed profile 50 cm thick to ensure initiation of vertical particle uplift. Very recently, investigators have warned that mini-tunnels and micro-tunnels are too small to develop acceptable boundary layer thickness and the results should not be scaled up to field scales due to this limitation (Fister and Ries, 2009).

Working section lengths of previous portable wind tunnel designs have varied from approximately 3 m (Gillette, 1978a; Fister and Ries, 2009) to almost 12 m (Houser and Nickling, 2001a, 2001b). The primary concern affecting design length is for adequate saltation to occur to reach near transport capacity. Raupach and Leys (1990) recommended adding saltating sand grains at the beginning of the working section. They offered the final criterion for their design, which was not truly aerodynamic but is listed below as criterion 6:

6. A portable wind tunnel simulation of erosion should allow for the introduction of saltating grains at the beginning of the working section if more than the very upwind area of an eroding field is to be simulated.

This criterion, they noted, raised even more questions as to design and operation of the tunnel, including how much material to introduce, what its size distribution should be, and how to distribute it realistically in the flow. Saltation has been shown to reach a maximum at about 7 m in wind tunnels (Shao and Raupach, 1992) and decreases thereafter, reaching an equilibrium at a distance between 10 m and 15 m (Maurer et al., 2006). Longer tunnels have limited utility in that they are less transportable (Fister and Ries, 2009) and require a substantially longer span of uniform level surface on which to be set (Sweeney et al., 2008).

We determined that we wanted our portable wind tunnel to be used to compare the erodibility of natural and disturbed surfaces and to generate representative dust emissions from

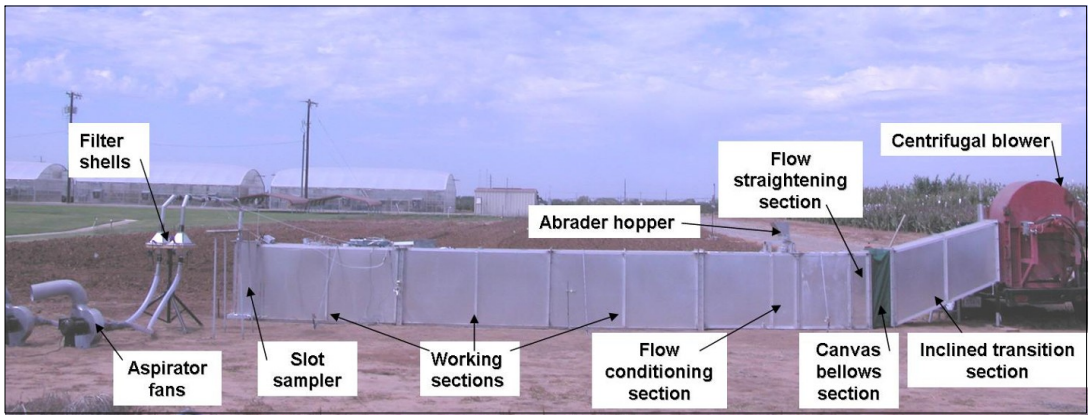

Figure 1. Picture of the portable wind tunnel in test configuration showing the integral airflow components.

the eroding surface that could be analyzed for chemical, physical, and biological characteristics. In addition to the design criteria discussed above, we added the following criteria.

- All surfaces coming into contact with the wind-eroded sediment must be aluminum to minimize any tunnel abrasion contamination of dust chemical contents (aluminum is ubiquitous in mineral soils and dusts and is therefore is a metallic constituent that is commonly ignored in dust analyses).
- The tunnel must be transportable using a standard-size pickup truck and tandem-axle trailer to facilitate access to remote areas and field research plots.
- All moving parts must be hydraulically driven to minimize the hazards posed by moving shafts or gears and chains.
- All parts other than the blower, flow-conditioning section, and the working section should be commonly available items that can be purchased near field locations.

CONSTRUCTION

A summary of the dimensions, maximum wind speed, and boundary layer thickness of our portable wind tunnel design may be found in table 1. A 5 m flat trailer with tandem axles was chosen for the construction platform. The trailer is built for hauling motor vehicles and is rated to carry 3,000 kg. The bed of the trailer is wood, allowing easy attachment of components and maintaining isolation of electrically operated components. Four pivoting hand-operated jacks were mounted on the corners of the trailer to allow height adjustment and leveling on uneven surfaces. A full-length perspective of the portable wind tunnel and its respective parts is presented in figure 1.

We used the same centrifugal blower that Fryrear (1984, 1985) had previously used. The cage diameter is approximately 1 m, and the impellers are rear-facing. This blower is capable of producing 9.36 m^3 s^{-1} of airflow at a maximum 525 rpm and against a 2.5 kPa pressure increase. Given the 0.5 m^2 cross-section of the wind tunnel, this allows for a maximum mean wind speed of 18.7 m s^{-1}. Full power requirement for fan operation is 9.5 kW. The fan is set in a custom welded steel frame that is mounted using a 5 cm diameter pin to a low-friction turntable on the left rear of the trailer. This turntable arrangement allows the fan outlet to face either the left side or the rear of the trailer in the operation configuration or to the center of the trailer for transport.

The bottom of the fan outlet is approximately 0.5 m above the surface of the ground when the trailer is level. The fan outlet is approximately 60 cm wide and 80 cm tall. These are slightly different dimensions from the dimensions chosen for the working section of the tunnel, but the cross-sectional area is very similar. In order to move the flow duct closer to the soil surface and to adapt the duct area to the dimensions of the flow-conditioning and working sections, an inclined transition section was built that brought the flow to within 5 cm of the ground and to a final dimension of 0.5 m wide and 1 m tall. The 0.5 m wide and 1 m tall dimensions are consistent throughout the remainder of the portable tunnel. This transition section is built with a frame of 4 cm aluminum angle, 0.5 cm thick, and skinned with 0.75 mm sheet aluminum that is attached to the inside of the frame with aluminum pop rivets. The mounting flange for the transition section was mated to the fan outlet flange, marked, and drilled to facilitate connection using 10 mm diameter bolts 25 mm in length. All flanges of a given section are attached to the flanges of subsequent sections using similarly aligned holes and bolts.

The outlet of the inclined transition section is connected to a 40 cm canvas bellows section with flanges made from the aluminum angle at both ends. This bellows section is the final part of the transition section that allows fine adjustment of the duct height to very near the ground. The downstream flange connects to a 25 cm flow-straightening section with wire mesh diffuser screens and aluminum honeycomb (fig. 2). The diffuser screen serves to deflect flow from high-velocity sections of the duct to lower-velocity sections prior to entering the honeycomb. The honeycomb was custom ordered to have 19 mm hexagonal cells of 17 cm length. The length of the cells is 9.3 times the cell diameter, which is at the upper end of the recommended 5 to 10 times cell diameter for almost complete annihilation of the lateral components of turbulence. Lengths greater than 10 times the cell diameter tend to exert added drag along the length of the cell and induce secondary turbulence (Mehta, 1977; Mehta and Bradshaw, 1979).

The homogenized and straightened flow then enters a 2 m long flow-conditioning section (fig. 3) that is also built of a 4 cm aluminum angle frame and skinned inside the frame, including the floor, with 0.75 mm aluminum sheet. Waterproof abrasive cloth with 0.32 mm sand grains covers the flow-

Figure 2. Flow-straightening section showing the aluminum honeycomb.

conditioning section floor. The flow-conditioning section further modifies the flow by use of an optional replaceable frame that can be used to introduce flow trip fences and spires of user-defined heights, widths, and densities (Counihan, 1969; Irwin, 1981) to deepen the boundary layer. This feature allows for appropriate flow conditioning to simulate the flow over surfaces with longer aerodynamic roughness lengths before introduction of the flow over surfaces other than bare and flat. In addition, an abrader hopper holds sand, which can be controlled by means of replaceable orifice plates to regulate the rate of abrader dropped into inclined drop tubes. The orifice diameters and resulting rates of abrader flux are presented in table 2. The drop tubes are of an aerodynamic design to minimize flow disruption and still allow accelerated grains to strike the roughened floor and initiate saltation. These tubes are an accentuated teardrop or symmetric airfoil shape that allows a 10 mm round channel for unimpeded sand flow at the upwind end and 45 mm of straight surface from the edges of the 10 mm half-circle that join together at the downwind end to allow reattachment of the airflow and prevention of excessive turbulence. The inclined tubes are immediately downwind of the replaceable frame for optional trip fences and spires. The abrader material is dropped onto the flow-conditioning section floor approximately 1.5 m upwind of the soil surface to be tested. Upon striking the sandpaper surface, the abrader, with vertical and horizontal momentum, immediately begins to saltate, resulting in a fully developed saltation field prior to entering the test section.

The working section of the portable wind tunnel is composed of three identical sections of 2 m each, allowing for assembled lengths of from 2 m to 6 m. The individual sections are composed of an aluminum frame built with 4 cm angle and skinned with 0.75 mm sheet aluminum inside the frame. The frame is constructed so that slightly less than 1 m of aluminum sheet is exposed between rigid frame members, allowing for a lightweight but sturdy design. The edges of the working section contact the ground by means of interchangeable 4 cm aluminum angle edges that are 3 mm thick for tilled soils or 2.5 cm thick foam strips for crusted soils. Flexible grain-filled cloth tubes may also be used to seal the contact zone of the working section and the soil surface on the outside of the tunnel.

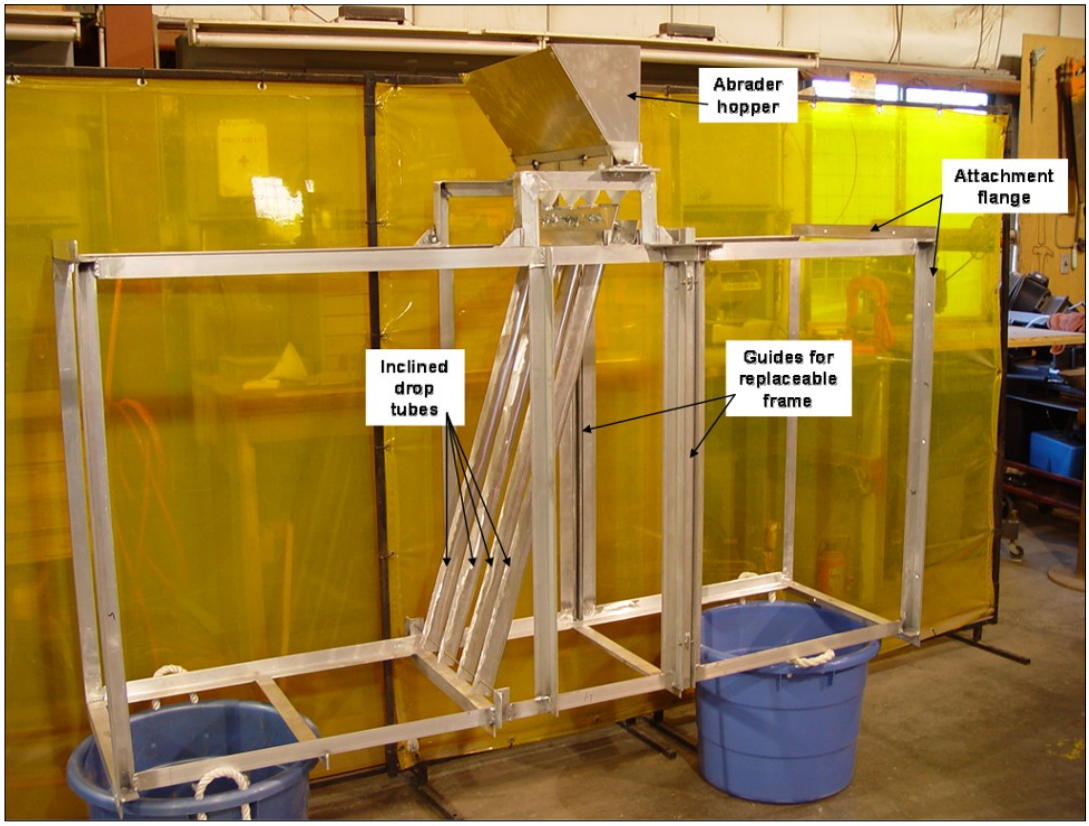

Figure 3. Flow-conditioning section prior to skin application showing the integral parts.

Table 2. Orifice diameters of the abrader hopper orifice plates and measured abrader flux rates.

Orifice Diameter (mm)	Abrader Flux Rate (kg m^{-1} s^{-1})
1.59	0.001
2.38	0.003
3.18	0.007
3.57	0.011
3.97	0.015
4.37	0.020
4.76	0.028
5.16	0.033
5.56	0.042
5.95	0.053

The main blower is powered by a hydraulic motor with a 1 L s^{-1} (16 GPM) flow rate at 550 rpm (Haldex FM 30) and regulated with a flow divider (Prince RD 150 16) (fig. 4a). The water pump (Dayton 2ZWY9) for the hydraulic oil heat exchanger, and a 12 VDC electric alternator (Leece Neville LN/110-555PHO) are driven by hydraulic motors (Haldex 1070054) each controlled by a flow regulating valve (Parker F400 S). The hydraulic motors are actuated with a full detent three-spool valve body with integral adjustable pressure regulator (Prince RD 2575T4EDA1). The high-pressure side of the hydraulic system consists of a hydraulic pump capable of producing 1.5 L s^{-1} of flow at 10.5 MPa (Haldex W1500), the valve body with pressure relief valve, and the three hydraulic motors mentioned above controlled with flow controllers and dividers. Downstream of the motors, the low-pressure system consists of a water-cooled heat exchanger capable of removing 27 kW of heat from the hydraulic oil at the design oil flow rate (Lovejoy 8457103313), a filter (Parker 50AT03CN15 BBH), and a 38 L horizontal reservoir (LDI VQ47900) with a filtering breather cap (LDI 5216) (fig 4b). A 6-cylinder horizontally opposed motorcycle engine with 1.5 L displacement and 74.6 kW output at 5200 rpm (Honda GL 1500) provides the motive force for the hydraulic pump. The engine is integrated with a 5-speed manual transmission and driveshaft output that connects to the input shaft for the pump. Three fan-aspirated water-cooling radiators, one for the hydraulic oil heat exchanger (Nissan auto radiator, Silla 7167A) radiator and two for the engine (Nissan auto radiator, Silla 7167A; and Ford truck radiator, Silla 2171A) dissipate heat from a gasoline burn rate of 19 L h^{-1} (fig. 4c). The schematic of the non-engine (radiator fan) charging and electrical system is presented in figure 4d.

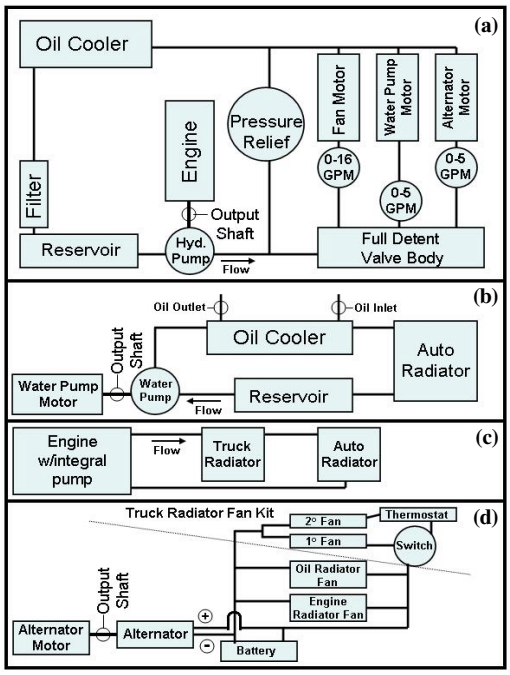

Figure 4. System schematics for the (a) hydraulic drive system, (b) hydraulic oil cooling system, (c) engine cooling system, and (d) non-engine charging and electrical system.

INSTRUMENTATION

Tunnel wind speed is determined by use of a hot-wire anemometer located at the beginning of the working section at 50 cm height above the surface. This anemometer is connected to a Campbell Scientific CR23X datalogger for conversion of the signal to wind speed in m s^{-1}. The wind speed is monitored at a rate of 1 Hz. An isokinetically aspirated vertical slot sampler (Hagen, 2001; Amante-Orozco and Zobeck, 2002) with a 3 mm wide mouth spans the vertical 1 m height of the tunnel (fig. 5). The opening and intake section of the slot sampler runs over a screened floor into a 12.5 cm vertical vortex with a funnel at the bottom to drop the creep- and saltation-sized sediments into a segmented collection pan. Pressure tubes at 5, 10, 15, 30, and 55 cm above the surface allow matching of the wind speed profile at the tunnel exit and within the sampler for monitoring the integrated wind speed profile to ensure and facilitate adjustment for isokinetic flow. Fine flow adjustments (approximating the logarithmic wind flow profile) are made by raising and lowering the aspirator tube. This is done only once for each target wind speed.

Within the vertical slot sampler, suspended sediment is aspirated through a 5 cm (2 in.) diameter tube containing a pitot tube connected to a 0 to 622.5 Pa differential pressure transducer. The pressure transducer's electrical output is connected to the datalogger, and the data are used to estimate the total volume aspirated in a discrete period of time. The flow in the aspirated tube is connected to a Y-shaped flow splitter that feeds the flow to two filter shells, each containing a 20 cm × 25 cm glass fiber filter. The filter shells are aspirated with an electrically powered centrifugal regenerative blower. A 5 kW gasoline-powered 250 VAC generator provides the power to run the blower motor. The filters and trapped sediment provide an integrated measure of suspended sediment evolving from the eroding surface. Temporal patterns of dust evolution are isokinetically sampled from the pre-filter flow stream, analyzed, and recorded with a GRIMM Technologies 1.108 particle size spectrometer once each 6 s throughout the period of the test. The GRIMM spectrometer records the number of particles in 16 different size classes and allows a time series of USEPA-regulated PM_{10} and $PM_{2.5}$ emissions to be measured. In general, the data from the GRIMM spectrometer is related to the data from the filters by a scaling factor that varies with the particle size distribution of the surface soil.

Saltation activity is monitored using a Sensit impact sensor (Stockton and Gillette, 1990) horizontally mounted so that the center of the piezoelectric element is 5 cm above the surface. Counts per second are recorded during the initial

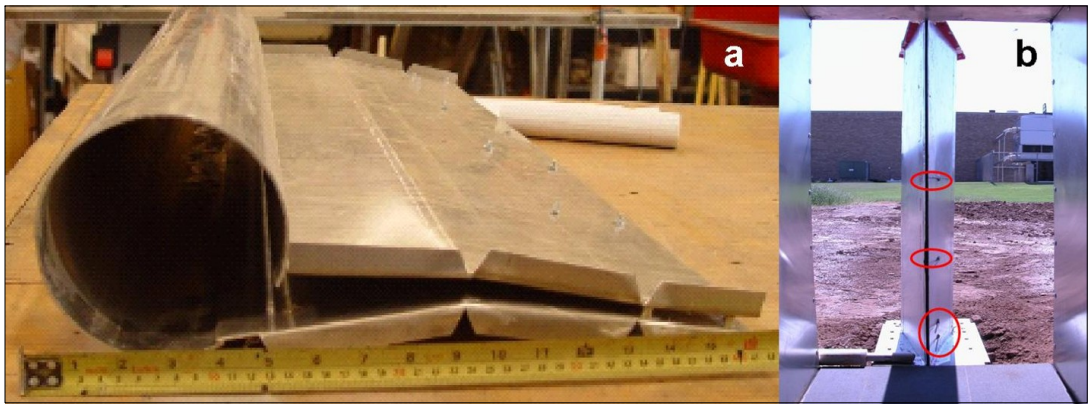

Figure 5. Isokinetic slot sampler showing (a) the cross section of flow and basic construction and (b) the fully assembled slot sampler deployed at the mouth of the tunnel. The circles highlight the positions of the pitot tubes.

increase of tunnel wind speed to allow estimation of saltation seconds (Stout, 2004) and thus the threshold velocity of the surface. During the remainder of the test, the data from the Sensit are used to assess temporal uniformity of saltation and abrader flux.

Operation and Calibration of the Portable Wind Tunnel

Following completion, the portable wind tunnel underwent several months of calibration and validation. During this time, standard operating procedures were developed and instrumentation added or adjusted as necessary to obtain a reliable and descriptive data stream. The working section of the tunnel was fitted with a plywood floor that was covered in 0.4 mm sand diameter sandpaper to eliminate anisotropic soil surfaces from affecting the calibration procedures and data. Aluminum frames with 10 mm holes at 10 cm intervals in each side were installed between the flow-conditioning section and the first working section to allow sampling of the air velocity in a two-dimensional array normal to the direction of flow. The same sampling procedure was also employed between the second and third tunnel working sections 4 m downwind of the first array. Wind speeds were sampled with a hot-wire anemometer (Kurz 430DC) that had been modified to include a 1 m distance between the controller and the probe tip.

The first calibration procedure was to adjust the wire mesh diffuser screens in the flow-straightening section to obtain a logarithmic wind speed profile that would be expected over a smooth, flat surface. This is an iterative process requiring multiple cycles of blower operation, collecting mean wind speeds from both arrays, analyzing the data, and adding, removing, or trimming screen sections to approach an ideal profile at the beginning of the working section that was subsequently maintained through the rest of the tunnel. Diffuser screen with a 10 mm mesh was used for this operation, and screen was added where the velocity was greater than desired and removed or trimmed where the velocity was less than desired. The velocity profile established for normal operation was one that would extrapolate to a mean wind speed of 15 m s^{-1} at a height of 2 m and for which the velocity was 12.6 m s^{-1} at the 0.5 m height on the centerline of the tunnel. This mean wind speed would represent a moderately intense aeolian event and was expected to result in erosion of most erodible surfaces. The 2 m wind speed target interpolated to a tunnel centerline wind speed of 12.6 m s^{-1} at a height of 0.5 m. This tunnel centerline wind speed resulted in a Froude number (eq. 2) of 16.5, well in the middle of the range of upper limits proposed by previous researchers (White and Mounla, 1991; Pietersma et al., 1996). The wind speed profiles before calibration and the theoretical ideal are presented in figure 6a, the wind speed

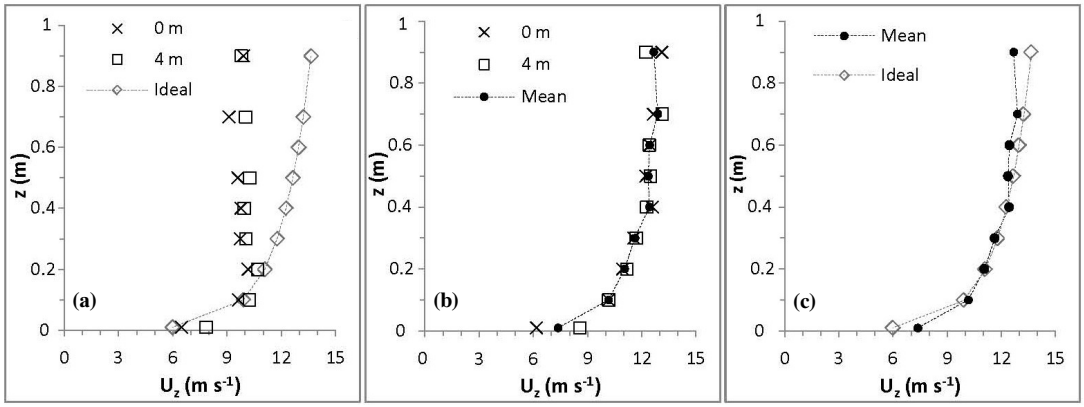

Figure 6. Centerline wind speed profiles: (a) idealized wind speed profile over a smooth sand surface and the original wind speed profile before calibration, (b) wind speed profiles after calibration at the 0 m and 4 m distances in the test section of the wind tunnel and the mean wind speed profile, and (c) mean wind speed profile and the idealized wind speed profile.

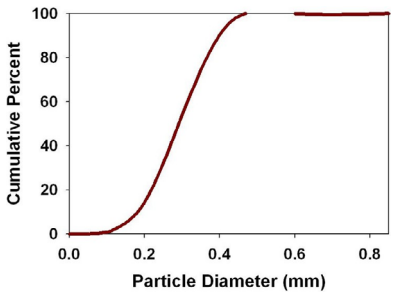

Figure 7. Cumulative size distribution for the abrader sand used in the portable wind tunnel.

profile we developed and measured after adjustment and calibration for both working section arrays are presented in figure 6b, and a comparison of the mean wind speed profile for both working section arrays is compared with the ideal wind speed profile in figure 6c.

From the wind speed profile, a boundary layer thickness may be estimated. Schlichting and Gertsen (2000) stated that boundary layer thickness is a poorly defined concept and recommended using a determining factor of the height at which the logarithmic wind speed profile attains 99% of its maximum value. By using this criterion, we estimate that the boundary layer thickness in our working section is approximately 0.5 m, the value recommended by Maurer et al. (2006) and deeper than that reported for any previous portable wind tunnel other than the very large design of Pietersma et al (1996). The observed maximum wind velocity observed 4 m down the working section was found at the 0.7 m height, and the actual boundary layer thickness may be greater. However, due to the slight decrease in mean velocity observed at the 0.6 m height, we are using the more conservative estimate of boundary layer thickness.

For the input abrader material, we chose quartz sand with very low amounts of surface coatings and low extractable metals and plant nutrients. The particle size distribution is presented in figure 7, and the extractable chemicals are presented in table 3. The very narrow range of particle sizes is similar to naturally occurring abrader sand on many loam soils and may facilitate separation of the native soil from the introduced abrader in fine-textured soils. The very low levels of extractable chemicals in the sand minimize the introduced abrader effects in the chemical analyses of the suspended sediments.

The second calibration procedure was to measure the mass of quartz abrader dropping through the holes of each of the orifice plates for a period of 5 min to determine the rate of abrader flux for each diameter hole (table 2). For most tests of soil surfaces, we chose the abrader flux rate closest to 0.01 kg m^{-1} s^{-1}, similar to field-measured data for natural sand movement (Namikas, 2003). This rate may be doubled or trebled for simulation of intense storms. During the calibration process, the vertical slot sampler was found to be 73% efficient (Cox, 2009) at capturing the vertical profile of saltation-introduced abrader. The efficiency may be greater for erosion on natural surfaces where the saltation and suspended sediment (dust) occupies more of the 1 m sampling integration depth.

Table 3. Extractable chemical constituents of abrader sand used with the portable wind tunnel.

Constituent	Percent
SiO_2 (silicon dioxide)	99.66
Fe_2O_3 (iron oxide)	0.02
Al_2O_3 (aluminum oxide)	0.07
TiO_2 (titanium oxide)	0.01
CaO (calcium oxide)	0.01
MgO (magnesium oxide)	0.01
Na_2O (sodium oxide)	0.01
K_2O (potassium oxide)	0.01
LOI (loss on ignition)	0.20

Summary and Conclusions

We built a portable boundary layer wind tunnel for field research using readily available materials. The tunnel is self-contained and mounted on a 5 m tandem trailer that can be pulled with a standard long-bed pickup truck. The 1 m tall and 0.5 m wide flow-conditioning and working sections allow for a maximum design wind speed of 18.7 m s^{-1}, although the tunnel is usually run at a lower wind speed that extrapolates to 15 m s^{-1} at 2 m above the ground and to 12.6 m s^{-1} at 0.5 m above the ground on the wind tunnel centerline. At this wind speed, the Froude number is between the upper limits proposed by previous researchers, and the boundary layer depth is approximately 50 cm. The length of the working section can be changed from 2 m to 6 m. A calibrated and adjustable abrader feeder allows saltation at the beginning of the working section. Sediment sampling is accomplished by a split flow that separates creep and saltation material from suspended sediment entering a vertically integrating iso-kinetic slot sampler.

This tunnel has been successfully field tested at ten locations in five states and has provided reliable and usable data. The soil surfaces tested have included tilled, tilled and rolled, naturally crusted, and artificially crusted with soil textures that have ranged from sandy loams through silt loams to clays on a playa surface and organic muck soils with varying percentages of minerals. The design is easily transported, assembled, and run with a crew of three. We anticipate that this tool will provide opportunities to test erodibilities and dust emission rates from numerous soils and soil and cropping management systems in the near future. Among other uses for this tunnel are collection of PM_{10} resulting from erosion of natural surfaces, abrasion of field-grown plants by saltating sand grains, and testing of soil additives to control saltation and dust emissions. Other researchers are encouraged to try these and other uses with this design and their modified designs.

References

Amante-Orozco, A., and T. M. Zobeck. 2002. Clay and carbonate effect on dust emissions as generated in a wind tunnel. In *Proc. ICAR5/GCTE-SEN Joint Conf.*, 83-86. J. A. Lee and T. M. Zobeck, eds. Publication 02-2. Lubbock, Tex.: Texas Tech University, International Center for Arid and Semiarid Lands Studies.

Armbrust, D. V., and J. E. Box, Jr. 1967. Design and operation of a portable soil-blowing wind tunnel. Pub. No. 41-131. Washington, D.C.: USDA-ARS.

Bagnold, R. A. 1941. *The Physics of Blown Sand and Desert Dunes*. London, U.K.: Methuen.

Baker, J. T. 2007. Cotton seedling abrasion and recovery from wind-blown sand. *Agron. J.* 99(2): 556-561.
Bennell, M. R., J. F. Leys, and H. A. Cleugh. 2007. Sandblasting damage of narrow-leaf lupin (*Lupinus angustifolius* L.): A wind tunnel simulation. *Australian J. Soil Res.* 45(2): 119-128.
Chandler, D. G., K. E. Saxton, and A. J. Busacca. 2005. Predicting wind erodibility of loessial soils in the Pacific Northwest by particle sizing. *Arid Land Res. Mgmt.* 19(1): 13-27.
Chepil, W. S. 1950. Properties of soil which influence wind erosion: I. The governing principle of surface roughness. *Soil Sci*. 69(2): 149-162.
Copeland, N. S., B. S. Sharratt, J. Q. Wu, R. B. Foltz, and J. H. Dooley. 2009. A wood-strand material for wind erosion control: Effects on total sediment loss, PM_{10} vertical flux, and PM_{10} loss. *J. Environ. Qual.* 38(1): 139-148.
Counihan, J. 1969. An improved method of simulating an atmospheric boundary layer in a wind tunnel. *Atmos. Environ.* 3(2): 197-214.
Cox, J. J. 2009. Field testing a portable wind tunnel for fine dust emissions. MS thesis. Lubbock, Tex.: Texas Tech University.
Fister, W., and J. B. Ries. 2009. Wind erosion in the central Ebro basin under changing land use management: Field experiments with a portable wind tunnel. *J. Arid Environ.* 73(11): 996-1004.
Fryrear, D. W. 1984. Soil ridges-clods and wind erosion. *Trans. ASAE* 27(2): 445-448.
Fryrear, D. W. 1985. Soil cover and wind erosion. *Trans. ASAE* 28(3): 781-784.
Gillette, D. A. 1978a. A wind tunnel simulation of the erosion of soil: Effect of soil texture, sandblasting, wind speed, and soil consolidation on dust production. *Atmos. Environ.* 12(8): 1735-1743.
Gillette, D. A. 1978b. Tests with a portable wind tunnel for determining wind erosion threshold velocities. *Atmos. Environ*. 12(12): 2309-2313.
Goossens, D., and Z. Y. Offer. 2000. Wind tunnel and field calibration of six aeolian dust samplers. *Atmos. Environ.* 34(7): 1043-1057.
Grini, A., G. Myhre, C. S. Zender, J. K. Sundet, and I. S. A. Isaksen. 2003. Model simulations of dust source and transport in the global troposphere: Effects of soil erodibility and wind speed variability. Institute Report Series No. 124. Norway, University of Oslo, Department of Geosciences.
Hagen, L. J. 2001. Assessment of wind erosion parameters using wind tunnels. In *Sustaining the Global Farm: Selected Papers from the 10th Intl. Soil Conservation Organization Meeting*, 742-746. D. E. Stott, R. H. Mohtar, and G. C. Steinhardt, eds. West, Lafayette, Ind.: Purdue University and the USDA-ARS National Soil Erosion Laboratory.
Hagen, L. J. 2004. Evaluation of the Wind Erosion Prediction System (WEPS) erosion submodel on cropland fields. *Environ. Modelling Software* 19(2): 171-176.
Hagen, L. J., L. E. Wagner, and E. L. Skidmore. 1999. Analytical solutions and sensitivity analyses for sediment transport in WEPS. *Trans. ASAE* 42(6): 1715-1721.
Houser, C. A., and W. G. Nickling. 2001a. The emission and vertical flux of particulate matter <10 μm from a disturbed clay-crusted surface. *Sedimentology* 48(2): 255-267.
Houser, C. A., and W. G. Nickling. 2001b. The factors influencing the abrasion efficiency of saltating grains on a clay-crusted playa. *Earth Surf. Proc. Landforms* 26(5): 491-505.
Huang, N., X. J. Zheng, Y. H. Zhou, and R. S. Van Pelt. 2006. Simulation of wind blown sand movement and probability density function of liftoff velocities of sand particles. *J. Geophys. Res.* 111: D20201. DOI: 10.1029/2005JD006559.
Irwin, H. P. A. H. 1981. The design of spires for wind simulation. *J. Wind Eng. Ind. Aerodynamics* 7(3): 361-366.
Kim, D. S., G. H. Cho, and B. R. White. 2000. A wind-tunnel study of atmospheric boundary-layer flow over vegetated surfaces to suppress PM_{10} emission on Owens (dry) Lake. *Boundary-Layer Meteorol.* 97(2): 309-329.
Kohake, D. J., E. L. Skidmore, and L. J. Hagen. 2010. Wind erodibility of organic soils. *SSSA J.* 74(1): 250-257.
Leys, J. F., and M. R. Raupach. 1991. Soil flux measurements using a portable wind erosion tunnel. *Australian J. Soil Res.* 29(4): 533-552.
Leys, J. F., and D. J. Eldridge. 1998. Influence of cryptogamic crust disturbance to wind erosion on sand and loam rangeland soils. *Earth Surf. Proc. Landforms* 23(11): 963-974.
Leys, J. F., C. Strong, G. H. McTainsh, S. Heidenreich, O. Pitts, and P. French. 2002. Relative dust emission estimated from a mini-wind tunnel. In *Proc. ICAR5/GCTE-SEN Joint Conf.*, 117-121. Publication 02-2. J. A. Lee and T. M. Zobeck, eds. Lubbock, Tex.: Texas Tech University, International Center for Arid and Semiarid Lands Studies.
Liu, L. Y., S. Y. Gao, P. J. Shi, X. Y. Li, and Z. B. Dong. 2003. Wind tunnel measurements of adobe abrasion by blown sand: profile characteristics in relation to wind velocity and sand flux. *J. Arid Environ.* 53(3): 351-363.
Macpherson, T., W. G. Nickling, and J. A. Gillies. 2008. Dust emissions from undisturbed and disturbed supply-limited desert surfaces. *J. Geophys. Res.* 113: F02S04. DOI: 10.1029/2007JF000800.
Maurer, T., L. Hermann, T. Gaiser, M. Mounkaila, and K. Stahr. 2006. A mobile wind tunnel for wind erosion field measurements. *J. Arid Environ.* 66(2): 257-271.
McKenna Neumann, C., and C. Maxwell. 1999. A wind tunnel study of the resilience of three fungal crusts to particle abrasion during aeolian sediment transport. *Catena* 38(2): 151-173.
Mehta, R. D. 1977. The aerodynamic design of blower tunnels with wide-angle diffusers. *Prog. Aerospace Sci.* 18: 59-120.
Mehta, R. D., and P. Bradshaw. 1979. Design rules for small low-speed wind tunnels. *Aeronaut. J.* 83: 443-449.
Namikas, S. L. 2003. Field measurement and numerical modeling of aeolian mass flux distribution on a sandy beach. *Sedimentology* 50(2): 303-326.
Nickling, W. G., and J. A. Gillies. 1989. Emission of fine-grained particulates from desert soils. In *Paleoclimatology and Paleometeorology: Modern and Past Patterns of Global Atmospheric Transport, Series C: Mathematical and Physical Sciences*, 282: 133-165. M. Leinen and M. Sarnthein, eds. Dordrecht, The Netherlands: Kluwer Academic.
Offer, Z. Y., and D. Goossens. 1995. Wind tunnel experiments and field measurements of aeolian dust deposition on conical hills. *Geomorphology* 14(1): 43-56.
Pietersma, D., L. D. Stetler, and K. E. Saxton. 1996. Design and aerodynamics of a portable wind tunnel for soil erosion and fugitive dust research. *Trans. ASAE* 39(6): 2075-2083.
Raupach, M. R., and J. F. Leys. 1990. Aerodynamics of a portable wind erosion tunnel for measuring soil erodibility by wind. *Australian J. Soil Res.* 28(2): 177-191.
Rice, M. A., and I. K. McEwan. 2001. Crust strength: A wind tunnel study of the effect of impact by saltating particles on cohesive soil surfaces. *Earth Surf. Proc. Landforms* 26(7): 721-733.
Roney, J. A., and B. R. White. 2006. Estimating fugitive dust emission rates using an environmental boundary layer wind tunnel. *Atmos. Environ.* 40(40): 7668-7685.
Saxton, K., D. Chandler, L. Stetler, B. Lamb., C. Claiborn, and B.-H. Lee. 2000. Wind erosion and fugitive dust fluxes on agricultural lands in the Pacific Northwest. *Trans. ASAE* 43(3): 623-630.
Schlichting, H., and K. Gersten. 2000. *Boundary Layer Theory.* Berlin, Heidelberg, New York, N.Y.: Springer-Verlag.
Shao, Y., and M. R. Raupach. 1992. The overshoot and equilibrium of saltation. *J. Geophys. Res.* 97 (D18): 20559-20564.
Sharratt, B. S. 2007. Instrumentation to quantify soil and PM_{10} flux using a portable wind tunnel. In *Proc. Intl. Symposium on Air*

Quality and Waste Management for Agriculture. ASABE Paper No. 701P0907cd. St. Joseph, Mich.: ASABE.

Stockton, P. H., and D. A. Gillette. 1990. Field measurement of the sheltering effect of vegetation on erodible land surfaces. *Land Degrad. Rehab*. 2(2): 77-85.

Stout, J. E. 2004. A method for establishing the critical threshold for aeolian transport in the field. *Earth Surf. Proc. Landforms* 29(10): 1195-1207.

Sweeney, M., V. Etyemezian, T. Macpherson, W. Nickling, J. Gillies, G. Nicolich, and E. McDonald. 2008. Comparison of PI-SWERL with dust emission measurements from straight-line wind tunnel. *J. Geophys. Res.* 113: F01012. DOI: 10.1029/2007JF000830.

Van Pelt, R. S., and T. M. Zobeck. 2007. Chemical constituents of fugitive dust. *Environ. Monit. Assess.* 130: 3-16.

Van Pelt, R. S., P. Peters, and S. Visser. 2009. Laboratory wind tunnel testing of three commonly used saltation impact sensors. *Aeolian Res.* 1(1-2): 55-62.

White, B. R., and H. Mounla. 1991. An experimental study of Froude number effect on wind tunnel saltation. In *Aeolian Grain Transport, Volume 1: Mechanics*, 145-157. O. E. Barndorff-Nielsen and B. B. Willets, eds. Acta Mechanica Supplementa 1. New York, N.Y.: Springer-Verlag.

Woodruff, N. P, and F. H. Siddoway. 1965. A wind erosion equation. *SSSA Proc.* 29(5): 602-608.

Zheng, X. J., N. Huang, and Y. H. Zhou. 2003. Laboratory measurement of electrification of wind-blown sands and simulation of its effect on sand saltation movement. *J. Geophys. Res.* 108(D10): 4322. DOI: 10.1029/2002JD002572.

Zingg, A. W. 1951a. A portable wind tunnel and dust collector developed to evaluate the erodibility of field surfaces. *Agron. J.* 43(2): 189-191.

Zingg, A. W. 1951b. Evaluation of the erodibility of field surfaces with a portable wind tunnel. *SSSA Proc.* 15(1): 11-17.

Zingg, A. W., and N. P. Woodruff. 1951. Calibration of a portable wind tunnel for the simple determination of roughness and drag on field surfaces. *Agron. J.* 43(2): 191-193.

Zobeck, T. M. 1991. Abrasion of crusted soils: Influence of abrader flux and soil properties. *SSSA J.* 55(4): 1091-1097.

Zobeck, T. M., and D. W. Fryrear. 1986. Chemical and physical characteristics of windblown sediment: II. Chemical characteristics and total soil and nutrient discharge. *Trans. ASAE* 29(4): 1037-1041.